The highly-connected MOFs constructed from nonanuclear and trinuclear lanthanide-carboxylate clusters: Selective gas adsorption and luminescent pH sensing

Yun-Jian Li,[†] Yu-Ling Wang,*[,†] and Qing-Yan Liu*[,†]

[†]*College of Chemistry and Chemical Engineering, Key Laboratory of Functional Small Organic Molecule of Ministry of Education, Jiangxi Normal University, Nanchang 330022, People's Republic of China*

Supporting Information

Table S1. Selected Bond Lengths (Å) of **JXNU-3**.[a]

Gd		Tb		Er	
Gd1−O1A	2.675(9)	Tb1−O1A	2.703(12)	Er1−O1A	2.749(15)
Gd1−O1	2.675(9)	Tb1−O1	2.703(12)	Er1−O1	2.749(15)
Gd1−O2	2.344(5)	Tb1−O2	2.343(8)	Er1−O2	2.276(7)
Gd1−O4	2.366(5)	Tb1−O4	2.373(7)	Er1−O4	2.329(6)
Gd1−O5	2.321(5)	Tb1−O5	2.329(6)	Er1−O5	2.257(6)
Gd1−O5A	2.321(5)	Tb1−O5A	2.329(6)	Er1−O5A	2.257(6)
Gd1−O9	2.570(6)	Tb1−O9	2.588(9)	Er1−O9	2.594(8)
Gd1−O13B	2.405(4)	Tb1−O13B	2.394(6)	Er1−O13B	2.316(5)
Gd1−O13C	2.405(4)	Tb1−O13C	2.394(6)	Er1−O13C	2.316(5)
Gd2−O1	2.392(5)	Tb2−O1	2.394(8)	Er2−O1	2.320(8)
Gd2−O1D	2.415(6)	Tb2−O1D	2.385(8)	Er2−O1D	2.367(9)
Gd2−O1W	2.338(9)	Tb2−O1W	2.326(13)	Er2−O1W	2.297(13)
Gd2−O2	2.337(3)	Tb2−O2	2.343(4)	Er2−O2	2.309(4)

Gd2−O3	2.3206(12)	Tb2−O3	2.3158(17)	Er2−O3	2.2798(19)
Gd2−O4D	2.331(3)	Tb2−O4D	2.330(4)	Er2−O4D	2.286(3)
Gd2−O6D	2.335(5)	Tb2−O6D	2.309(7)	Er2−O6D	2.273(6)
Gd2−O12B	2.285(5)	Tb2−O12B	2.315(8)	Er2−O12B	2.251(7)
Gd3−O2W	2.367(7)	Tb3−O2W	2.413(13)	Er3−O2W	2.313(11)
Gd3−O7	2.3912(4)	Tb3−O7	2.3764(6)	Er3−O7	2.3725(5)
Gd3−O8	2.332(7)	Tb3−O8	2.331(11)	Er3−O8	2.280(10)
Gd3−O10F	2.315(5)	Tb3−O10F	2.318(8)	Er3−O10F	2.260(7)
Gd3−O10G	2.315(5)	Tb3−O10G	2.318(8)	Er3−O10G	2.260(7)
Gd3−O11H	2.306(5)	Tb3−O11H	2.294(7)	Er3−O11H	2.253(6)
Gd3−O11E	2.306(5)	Tb3−O11E	2.294(7)	Er3−O11E	2.253(6)

[a] symmetry Codes, A: + *x*, + *y*, 3/2 − *z*; B: 1 + *y* − *x*, 1 − *x*, 3/2 − *z*; C: 1 + *y* − *x*, 1 − *x*, + *z*; D: 2 − *y*, 1 + *x* − *y*, + *z*; E: 1 − *y* + *x*, 1 − *y*, 1 − *z*; F: + *y*, + *x*, 1/2 + *z*; G: + *y*, + *x*, 1 − *z*; H: 1 − *y* + *x*, 1 − *y*, 1/2 + *z*.

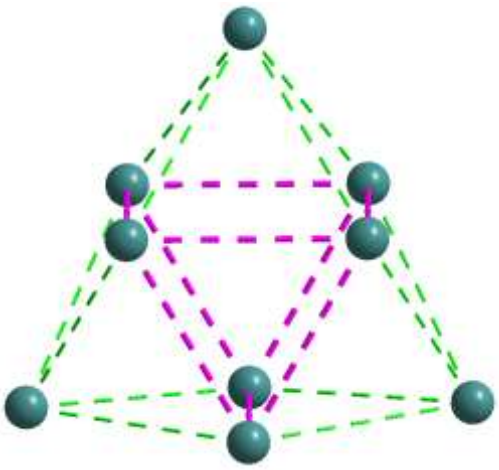

Figure S1. The nine lanthanide ions in the $[Ln_9(\mu_3\text{-}O)_2(\mu_3\text{-}OH)_{12}(CO_2–)_{12}(HCO_2)_3(H_2O)_6]$ cluster form a tricapped trigonal prism arrangement.

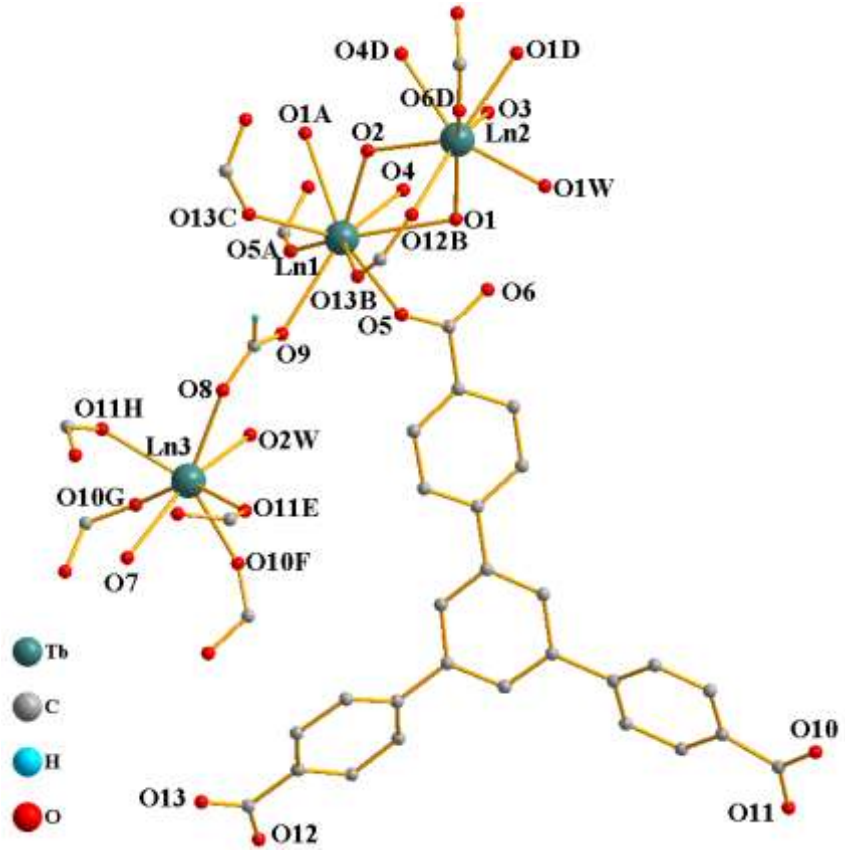

Figure S2. Coordination environments of Ln^{3+} ions in **JXNU-3**.

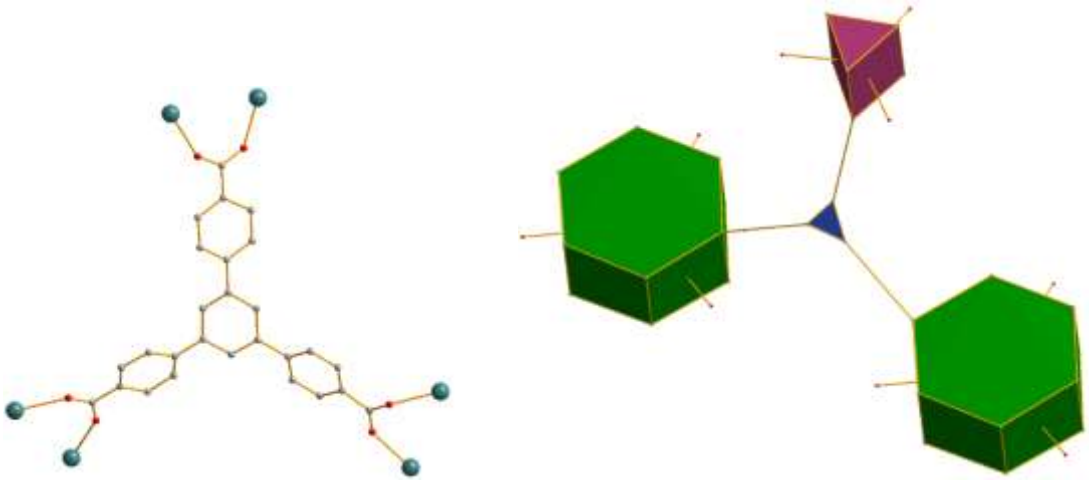

Figure S3. Coordination mode of the BTB ligand (left) and each BTB ligand links two nonanuclear $[Ln_9(\mu_3\text{-}O)_2(\mu_3\text{-}OH)_{12}(O_2C\text{–})_{12}(HCO_2)_3(H_2O)_6]$ clusters and one trinuclear $(Ln_3(\mu_3\text{-}O)(O_2C\text{–})_6(HCO_2)_3(H_2O)_3]$ cluster.

Topological Analysis:

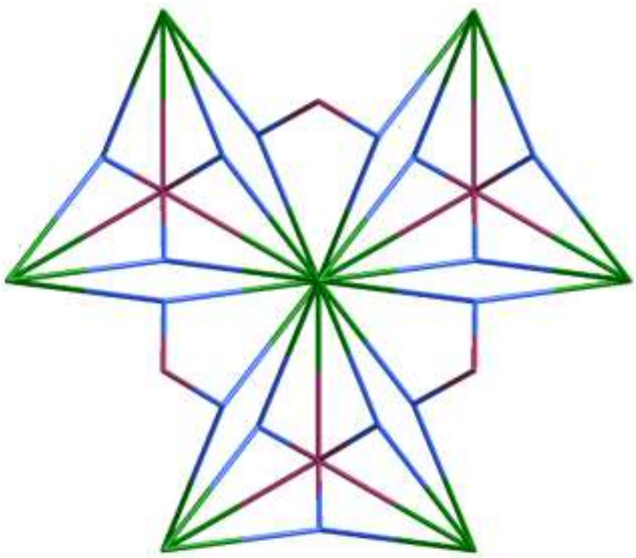

Figure S4. Topological analysis of **JXNU-3**, each 15-c node (green, nonanuclear cluster) is connected to three 9-c nodes (plum, trinuclear cluster) through three formate ligands and twelve 3-c nodes (blue, triangular organic ligand).

Prior to topological analysis, the structure has been simplified to its basic nodes (Fig. S4). The inorganic nonanuclear and trinuclear clusters are reduced to a 15-connected and 9-connected nodes (**α**, **β**), respectively, while the tritopic ligand is reduced to a 3-connected node (**γ**). The topological analysis reveals that the **JXNU-3** MOFs exhibits an unprecedented (3,9,15)-connected topology.

Point symbol for net: $(4^3)_6(4^9\cdot6^{18}\cdot8^9)(4^{24}\cdot6^{63}\cdot8^{18})$.[1]

(3,9,15)-c net with stoichiometry (3-c)6(9-c)(15-c); 3-nodal net; New topology.
TD10=3723.

Topological terms for each node:
(**α**) Point symbol: $\{4^{24}.6^{63}.8^{18}\}$
Extended point symbol:

[4.4.4.4.4.4.4.4.4.4.4.4.4.4.4.4.4.4.4.4.4.4.4.4.6.6.6.6.6.6.6.6.6.6.6.6.6.6.6.6.6(2).6(2).6(2).6(2).6(2).6(2).6(2).6(2).6(2).6(2).6(2).6(2).6(3).6(3).6(3).6(3).6(3).6(3).6(4).6(4).6(4).6(4).6(4).6(4).6(7).6(7).6(7).6(7).6(7).6(7).6(9).6(9).6(9).6(9).6(9).6(9).6(9).6(9).6(9).6(9).6(9).6(9).6(11).6(11).6(11).8(8).8(8).8(8).8(8).8(8).8(8).8(8).8(27).8(27).8(27).8(27).8(27).8(27).8(27).8(27).8(27).8(27).8(27).8(27)].

Coordination sequences: 15 30 89 158 261 342 491 650 843 990

(**β**) Point symbol: $\{4^9.6^{18}.8^9\}$

Extended point symbol:

[4.4.4.4.4.4.4(2).4(2).4(2).6(4).6(4).6(4).6(4).6(4).6(4).6(12).6(12).6(12).6(12).6(12).6(12).6(12).6(12).6(12).6(12).6(12).6(12).8(8).8(8).8(8).8(8).8(8).8(8).8(8).8(16).8(16).8(16)]

Coordination sequences: 9 42 87 146 243 366 501 626 813 1026.

(**γ**) Point symbol: $\{4^3\}$

Extended point symbol:

[4.4.4(2)]

Coordination sequences: 3 32 69 144 223 346 459 624 781 994.

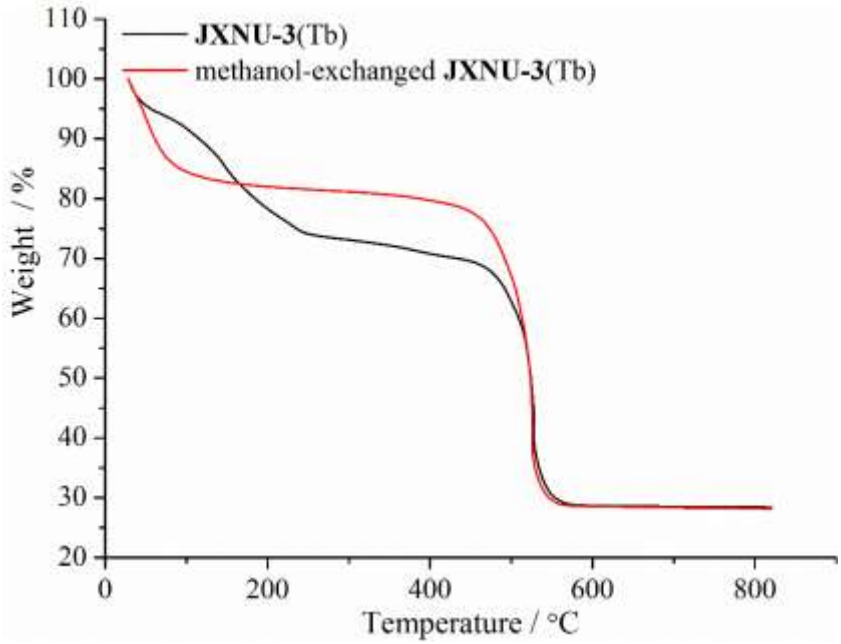

Figure S5. TGA curves for **JXNU-3**(Tb).

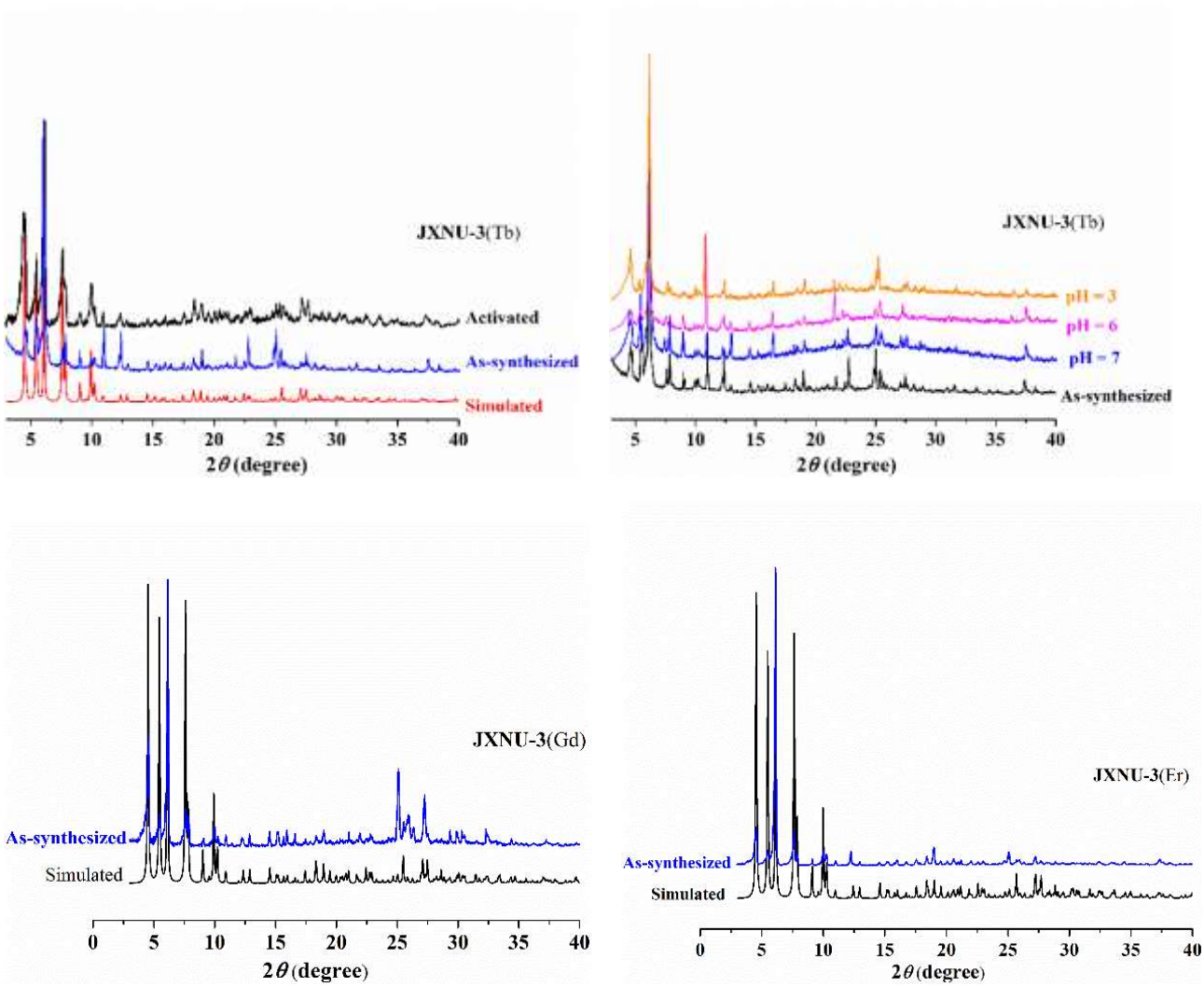

Figure S6. Powder X-ray diffraction patterns for **JXNU-3**.

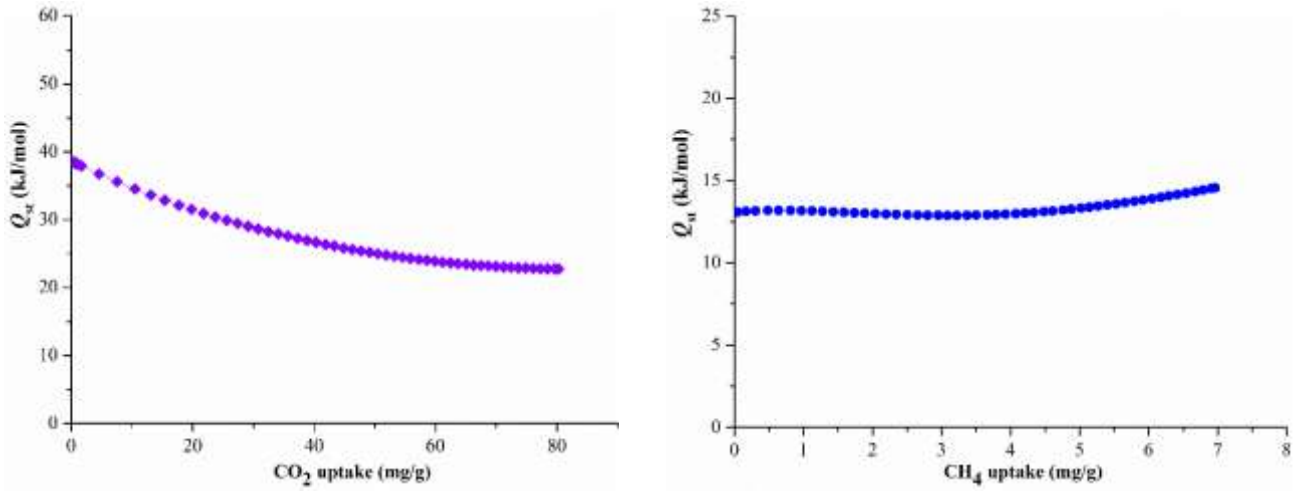

Figure S7. The enthalpy of adsorption (Q_{st}) as a function of CO_2 (left) and CH_4 (right) uptakes of **JXNU-3**(Tb)

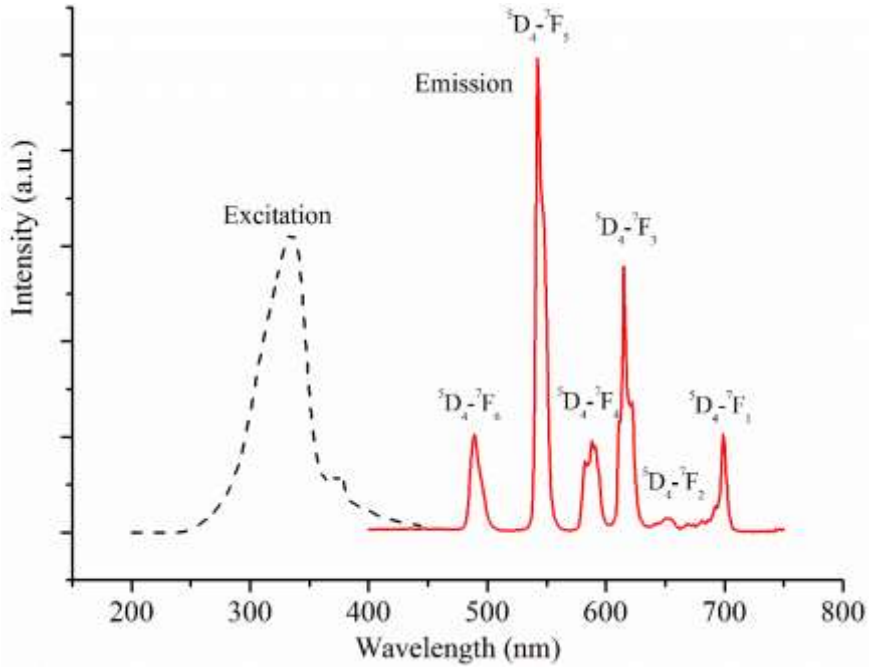

Figure S8. The excitation with emission monitored at a 544 nm and emission spectra for **JXNU-3**(Tb) (λ_{ex} = 327 nm) in the solid state.

Reference

1. Blatov, V. A.; Shevchenko, A. P.; Proserpio, D. M. Applied Topological Analysis of Crystal Structures with the Program Package ToposPro, *Cryst. Growth Des*. **2014**, *14*, 3576–3586.